



Title	Pressure dependence of local structure in liquid carbon disulfide
Author(s)	Yamamoto, Sekika; Ishibashi, Yasuhiko; Inamura, Yasuhiro et al.
Citation	The journal of chemical physics, 124(14), 144511 https://doi.org/10.1063/1.2185094
Issue Date	2006-04-14
Doc URL	https://hdl.handle.net/2115/8507
Rights	(c) 2006 American Institute of Physics
Type	journal article
File Information	JCP_124_14_144511.pdf



Pressure dependence of local structure in liquid carbon disulfide

Sekika Yamamoto^{a)} and Yasuhiko Ishibashi*Division of Physics, Graduate School of Science, Hokkaido University, N10W8, Sapporo 060-0810, Japan*Yasuhiro Inamura^{b)} and Yoshinori Katayama*Synchrotron Radiation Research Unit, Japan Atomic Energy Agency, Kouto 1-1-1, Sayo, Hyogo 679-5148, Japan*

Tomobumi Mishina and Jun'ichiro Nakahara

Division of Physics, Graduate School of Science, Hokkaido University, N10W8, Sapporo 060-0810, Japan

(Received 26 January 2006; accepted 14 February 2006; published online 14 April 2006)

High pressure x-ray diffraction measurements on liquid carbon disulfide up to 1.2 GPa are performed by using an energy dispersion method. The results are compared with a molecular dynamics calculation with usual Lennard-Jones potential. They give very good agreement for all pressures measured. It becomes clear that the liquid structure changes like hard core liquid up to the pressure just below crystallizing point. The relation between structural change and optical response at high pressure is discussed. © 2006 American Institute of Physics. [DOI: [10.1063/1.2185094](https://doi.org/10.1063/1.2185094)]

I. INTRODUCTION

Carbon disulfide is a simple linear molecule which exists as a liquid at room temperature and atmospheric pressure. It is known to crystallize in orthorhombic structure below 164 K under atmospheric pressure¹ and above 1.26 GPa at 293 K.² The carbon disulfide has a large optical polarizability and hence shows a large optical response. This property is utilized as several optical devices such as an optical Kerr shutter. The large optical response and its simple shape are also preferable for investigation of dynamical properties of liquids. For this purpose far infrared absorption,³⁻⁵ low frequency Raman scattering,^{6,7} transient optical Kerr effect,⁸⁻¹³ and impulsive stimulated scattering¹⁴ measurements have been done.

On the other hand, in investigation of liquid properties high pressure is a powerful tool because it can change the average molecular separation which affects the dynamical properties of molecules significantly. The pressure dependence of the dynamical properties of the carbon disulfide has been investigated in recent ten years. It has been shown in these researches that the broad low frequency mode appears in Raman scattering spectrum and far infrared absorption spectrum shifts to higher frequency as the pressure is increased.^{4,6} This low frequency mode is sometimes regarded to originate in the librational motion of molecules.^{8,14}

The results of the measurements on the dynamical properties of liquids are sometimes compared with the theoretical results or computer simulations such as a molecular dynamics simulation. However, the interaction potentials used in these calculations are in many cases only justified at atmospheric pressure by comparing with diffraction data. This is mainly because of experimental difficulties in diffraction

measurements on liquids. The diffraction signals from liquids are usually very weak and the difficulty is more emphasized in high pressure experiments because it is usually done in a small pressure cell.

In recent years a highly intense synchrotron radiation light with continuous spectrum becomes available and it makes the diffractive investigation of such kind of materials under high pressure conditions possible. In this paper we will report on x-ray diffraction measurements on the liquid carbon disulfide under high pressures up to the pressure just below freezing point. The obtained structure functions are compared with the results from a molecular dynamics simulation and the change in the local structure of the liquid with pressure and its relation with the dynamics observed in optical measurements will be discussed.

II. EXPERIMENT

All measurements are done at beam line BL14B1 of SPring-8, Japan. The x-ray source is a synchrotron radiation beam from an 8 GeV storage ring. The high pressure apparatus is a cubic-type press which compresses a cubic pressure transmitting medium by six anvils. Each tungsten carbide anvil has a square flat of 10×10 mm². The specimen is placed in a Teflon capsule of 3 mm diameter and 3 mm long. Then the capsule is embedded in a cubic pressure transmitting medium which is made of 4:1 (by weight) mixture of amorphous boron and epoxy resin. The internal pressure calibrant of NaCl embedded in a BN capsule is placed at the lower part of the assembly. Diffraction signals are measured by an energy-dispersive method at room temperature using a liquid nitrogen-cooled Ge solid state detector. Diffraction measurements are performed at fixed scattering angles of 4°, 5°, 6°, 8°, 10°, 13°, 16°, and 20° in order to obtain $S(k)$ on a wide k scale.

Several corrections are applied to the intensity spectra obtained at each angle. First, a background spectrum measured using an empty cell at atmospheric pressure are sub-

^{a)}Electronic mail: sekika@optphys.sci.hokudai.ac.jp^{b)}Present address: Neutron Radiation Laboratory, Institute for Solid State Physics, University of Tokyo, Kashiwanoha 5-1-5, Kashiwa, Chiba 277-8581, Japan.

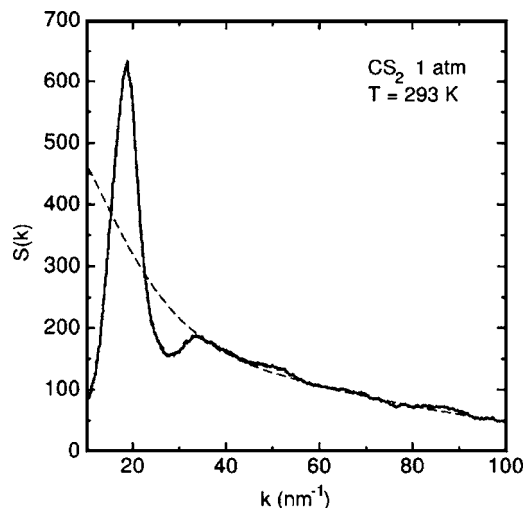


FIG. 1. Structure function of liquid carbon disulfide obtained at room temperature and atmospheric pressure.

tracted. Then a pulse pileup correction,^{15,16} an escape correction,^{17,18} and a slit correction¹⁷ are applied according to the literature. Corrected spectra are then processed by a Monte Carlo calculation that was originally developed by Funakoshi¹⁹ to obtain structure functions. In the calculation an effective incident beam spectrum is determined to minimize the difference in the structure functions obtained at different angles. Subtraction of Compton scattering and intensity normalization using the Norman–Krogh–Moe method^{20,21} are also included in the program.

III. EXPERIMENTAL RESULTS

The structure function of liquids per one molecule can be expressed as a sum of an atomic scattering term $S_a(k)$ and an interference term $S_i(k)$. The atomic term $S_a(k)$ is independent of liquid structure and calculated as

$$S_a(k) = \sum_{\alpha} f_{\alpha}^2(k),$$

where $f_{\alpha}(k)$ is an atomic scattering factor which is tabulated in “International Tables for Crystallography,”²² and α is an index for the atoms in a molecule. The interference term $S_i(k)$ is expressed as

$$S_i(k) = \sum_{\alpha, \beta} f_{\alpha}(k) f_{\beta}(k) \int_0^{\infty} 4\pi r^2 \rho_{\alpha\beta} \{g_{\alpha\beta}(r) - 1\} \frac{\sin kr}{kr} dr, \quad (1)$$

where $\rho_{\alpha\beta}$ is an averaged pair density of atomic species α and β , $g_{\alpha\beta}(r)$ is a pair distribution function (PDF), which gives the relative probability that an atom α finds an atom β at a distance r . The $g_{\alpha\beta}(r)$ is normalized to give unity at large r .

In Fig. 1 we show an obtained structure function of the liquid carbon disulfide at room temperature and atmospheric pressure together with the calculated $S_a(k)$. We can obtain interference term $S_i(k)$ by subtracting $S_a(k)$ from the obtained structure function. However, it is hard to calculate exact pair distribution functions $g_{\alpha\beta}(k)$ only from $S_i(k)$ be-

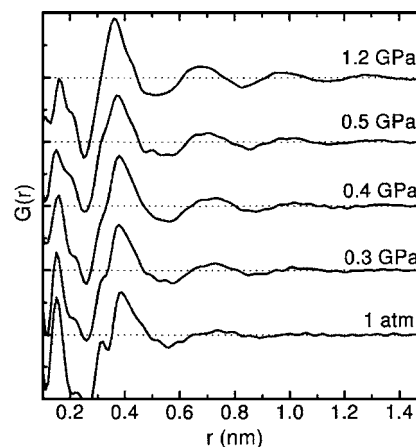


FIG. 2. Radial distribution function $G(r)$ obtained using Eq. (2) for various pressures.

cause the separation of the contribution of each atomic pair is difficult. Therefore we employ the method described in the reference²³ to deduce the radial distribution function. We calculate the function,

$$G(r) = 1 + \frac{1}{2\pi^2 \rho r} \int_0^{\infty} k M(k) S_i(k) \sin kr dk, \quad (2)$$

where

$$M(k) = \left[\sum_{\alpha} f_{\alpha}(k) \right]^{-2}, \quad (3)$$

and ρ the density of the liquid. The distribution function $G(r)$ gives unity at large r and includes the contribution of all pair distribution functions approximately weighed by the atomic scattering factor $f_{\alpha}(k) f_{\beta}(k)$. In carbon disulfide the atomic scattering factor of sulfur is much larger than that of carbon and therefore $G(r)$ is dominated by sulfur-sulfur contribution.

The conversion results are shown in Fig. 2. The peaks at $r=0.16$ nm and $r=0.31$ nm are the intramolecular sulfur-carbon and sulfur-sulfur peaks, respectively. The intensities of these peaks decrease with pressure because $G(r)$ is normalized to give unity at long distance where the intensity reflects the average density of the liquid which increases with pressure while the intramolecular pair density per molecule is constant. The structure between these peaks is a kind of ghost caused by abrupt termination in the Fourier transformation of Eq. (2). The intramolecular distance is regarded as almost independent of pressure²⁴ and the slight shift of sulfur-carbon peak seen at 0.5 GPa will be the error caused by the ghost.

We see the first intermolecular peak at $r=0.4$ nm grows with pressure. Also the succeeding oscillation of the density becomes clearer at high pressures. These changes appear in $S(k)$ as a growth and narrowing of the peak at $k \sim 20$ nm⁻¹. The peak for intramolecular sulfur-sulfur at $r=0.31$ nm distance merges with the first intermolecular peak at high pressures, indicating that the sulfur-sulfur distance between adjacent molecules approaches to intramolecule sulfur-sulfur distance.

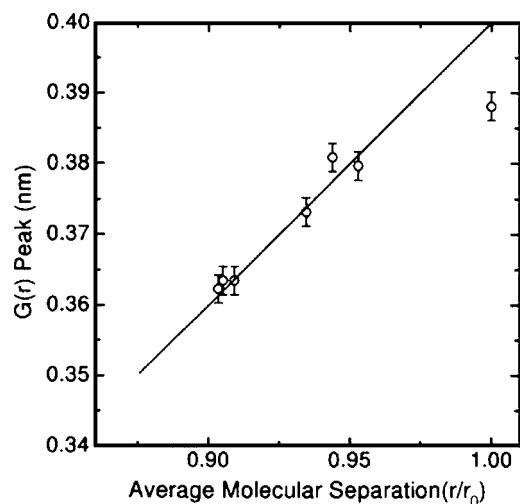


FIG. 3. First intermolecular peak of $G(r)$ plotted against the average molecular separation r relative to the atmospheric value r_0 . The solid line shows a proportional dependence on r .

The pressure dependence of the first intermolecular peak is shown in Fig. 3 as a function of average molecular separation relative to the separation at atmospheric pressure (r_0). The average separation for each pressure is calculated from the corresponding molecular density reported in the reference.^{25,26} The linear solid line shows the proportional dependence on r/r_0 . The $G(r)$ peak depends almost proportionally on the average molecular separation below $r/r_0 = 0.95$ which corresponds to 0.3 GPa in pressure. It is known that the van der Waals diameter of sulfur (~ 0.35 nm) is larger than that of carbon (~ 0.30 nm).²³ As a result, when the liquid is relatively sparse the CS₂ molecules will change the local configuration so as to avoid the sulfur-sulfur contact and make the sulfur-carbon distance closer. But if the liquid becomes so dense that the molecules no longer have extra space to avoid the contact, the intermolecular atomic distance must be shortened as the pressure is applied. In this case the nearest sulfur-sulfur distance will change rather linearly with average molecular separation. Therefore it is deduced from the pressure dependence of $G(r)$ peak that the significant change in the liquid structure occurs below 0.3 GPa and after that the structural change mainly occurs in the interatomic distance.

IV. COMPARISON WITH MD SIMULATION

The molecular dynamics (MD) calculations are performed at several pressures. The program used is GROMACS version 3.2.1.^{27,28} We use a rigid molecule model which utilizes a dummy atom configuration described in its manual. For the intermolecular potential a site-to-site Lennard-Jones (LJ) potential used by Zhu *et al.*²⁹ is used. Partial charges of $q_C = -0.308e$ and $q_S = 0.154e$ are added to each atomic site to reproduce a quadrupole moment.²⁹ The box dimension is chosen to $4 \times 4 \times 4$ nm³ with cyclic boundary condition and the number of molecules at each pressure is selected to realize the corresponding density which is experimentally determined in the literature.^{25,26} For example, those are 636 molecules at atmospheric pressure, and 850 molecules at

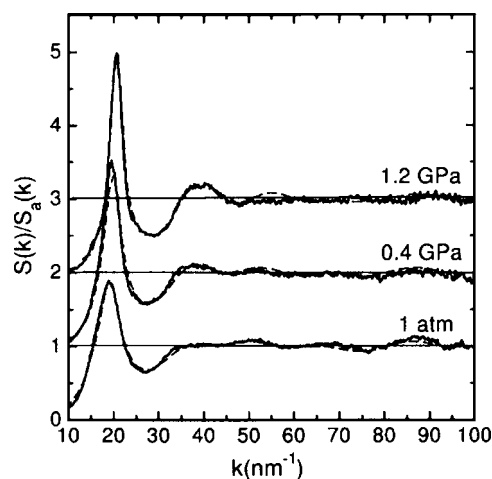


FIG. 4. Comparison of the structure functions obtained from x-ray diffraction experiments (solid lines) with MD simulation (dashed lines) at each pressure.

1.2 GPa. The interaction cutoff distance is chosen to half the box size. For every pressure the molecules are distributed randomly and a succeeding energy minimization is applied to determine starting configuration. For the energy minimization a steepest descent method included in the program is used. After the starting configuration is determined the main part of the simulation is performed under constant box size and constant temperature of 293 K. The time step is chosen to 0.5 fs. We monitor a total energy and a pressure value reported by the program to confirm the achievement of the thermal equilibrium and it takes about 30 000 step (15 ps) to reach the equilibrium at 1.2 GPa. After the system fully reaches the thermal equilibrium, the structure is recorded six times at each 50 ps step. The pair distribution functions $g_{\alpha\beta}(r)$ are calculated from all atomic pairs in these structures and then the structure function is obtained using Eq. (1). The calculation results are shown in Fig. 4 for pressures of 1 atm, 0.4 GPa, and 1.2 GPa together with the experimental results. To emphasize high- k structure the structure functions are divided by $S_a(k)$. It is seen in the figure that the MD results reproduce the experimental structure function extremely well except for the small deviation around 55 nm⁻¹ seen at high pressures, indicating the applicability of the LJ potential at high pressures. The deviation around 55 nm⁻¹ have not been understood at this time and will be discussed in later section.

V. DISCUSSIONS

A. Liquid structure at high pressures

Figure 5 shows intermolecular pair distribution functions obtained from the MD calculation at atmospheric pressure and at 1.2 GPa. The solid, dashed, and dotted lines show sulfur-sulfur, sulfur-carbon, and carbon-carbon distributions, respectively. It is seen that the sulfur-sulfur PDF roughly reproduces most of the features of experimental $G(r)$, reflecting the dominance of sulfur scattering intensity. The PDF does not change significantly under pressure and indicates that the local structure at high pressure does not differ much from that at atmospheric pressure.

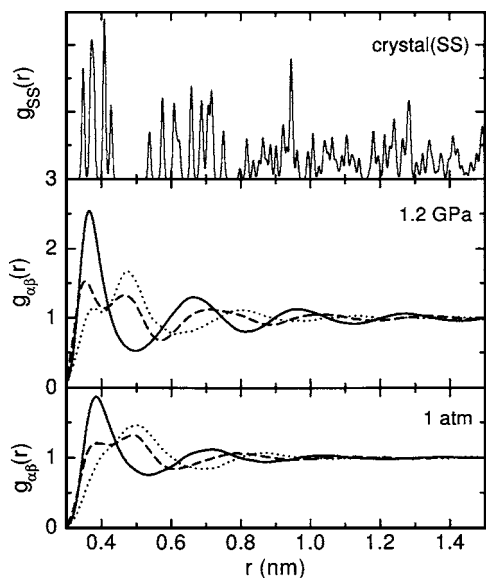


FIG. 5. Pair distribution functions calculated from MD simulation results and from the crystal structure at high pressure. The solid dashed, and dotted lines show sulfur-sulfur, sulfur-carbon, and carbon-carbon distributions, respectively. Only sulfur-sulfur distribution is shown for crystal.

It has been reported that the local structure of liquid carbon disulfide at atmospheric pressure can be approximated by a local crystal structure model.³⁰ Therefore we can compare the high pressure liquid structure with that of the crystal at high pressure. The high pressure crystal structure of carbon disulfide has an orthorhombic structure with the unit cell dimensions of $a=6.16$ Å, $b=5.38$ Å, and $c=8.53$ Å at $p=1.26$ GPa.² The molecules lie in bc plane and have a tilt about $\phi=41.5^\circ$ with respect to the b axis.^{31,32} According to this structure, there are four relative configurations for adjacent two molecules, as shown in Fig. 6. All atomic pair distances in PDF shorter than 0.6 nm come from these four configurations. We show the sulfur-sulfur PDF of high pressure crystal on top of Fig. 5. The peaks are shown broadened with narrow Gaussians for clarity. The first peak of $g_{SS}(r)$ for crystal phase around 0.4 nm consists of many peaks. These peaks include the contribution from all four configurations in Fig. 6. The overall distribution of the peaks resembles the liquid phase PDF and justifies the similarity of the structures of liquid and crystal.

If the liquid structure resembles to the crystal structure the closest sulfur-carbon peak at 0.35 nm in liquid $g_{\alpha\beta}(r)$ should correspond to T1 configuration and the closest carbon-carbon peak at 0.38 nm corresponds to P2 configuration. The second sulfur-carbon peak around 0.5 nm consists of all four configurations and the second carbon-carbon peak around 0.5 nm mainly comes from T1 and T2 configurations.

As the pressure is increased the first sulfur-carbon peak around 0.35 nm grows and shifts to shorter distance compared to sulfur-sulfur peak. This shows that the T1 configuration becomes more prominent and more perpendicular at high pressures. The parallel configuration P2 also

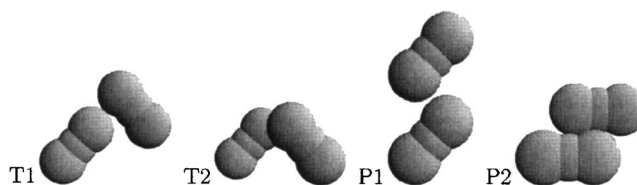


FIG. 6. Four configurations for adjacent molecules in crystal structure. In each configuration all atoms are on the same plane except for T2 configuration.

increases as indicated by the growth of carbon-carbon peak around 0.38 nm. The increase of the parallel configuration has been reported by several authors.^{3,33} But the distribution function tells us that the perpendicular configuration also grows with pressure. Therefore the molecules look to align each other like crystal as the pressure is increased.

On the other hand, we see in Fig. 5 that the first sulfur-sulfur peak for liquid PDF narrows with pressure although which is not prominent in total $G(r)$ because of the superposition of sulfur-carbon and carbon-carbon contributions (Fig. 2). The width of the first peak at 1.2 GPa is narrower than the sulfur-sulfur distribution around 0.4 nm in crystal PDF. This means that the liquid structure under pressure does not approach the exact crystal structure and keeps its hard core liquidlike structure. In hard core liquids the atomic separation approaches the sum of van der Waals radius of each atom as the pressure is raised because the space for their movement is getting restricted, while in the crystal structure the molecular ordering introduces a certain amount of distribution in the intermolecular atomic separation at the cost of interatomic potential. This will make the PDF of the liquid narrower than that of the crystal. In addition, the sulfur-sulfur distribution function at 1.2 GPa resembles to that of monoatomic liquids,³⁴ showing that the distribution function approaches that of hard-core monoatomic liquid as the sulfur-sulfur distance between adjacent molecules approaches the intramolecular sulfur-sulfur distance of 0.311 nm, as shown in Fig. 3. Therefore we should understand the molecular alignment shown above as the result of the structure change directed to the close-packed structure.

In MD section we mentioned the slight deviation between the experimental and calculated structure functions at around $k=55$ nm⁻¹. We made measurements three times at the same pressure and the structure around $k=55$ nm⁻¹ is fully reproduced. It is seen in Fig. 4 that the deviation is greater at higher pressure. For the explanation to the deviation there can be some possibility that at high pressure the molecules somewhat tend to align like crystal compared to the ideal hard core liquids although they are not simulated in the MD calculation. As shown in Fig. 5, the sulfur-sulfur distribution around $r=0.4$ nm is somewhat wider in crystal than in liquid. The interference between the peaks with broader distribution in k space can erase the oscillation in $S(k)$ at high- k region. Therefore the deviation may be interpreted as the slight structural deviation from the hard core liquid structure towards the crystal structure which is not simulated in MD calculation.

B. Comparison with optical measurements

In low frequency depolarized Raman scattering experiments on liquid carbon disulfide the peak energy of broad low frequency mode approaches that of crystal libration energy as pressure is increased.⁶ According to this result it is considered that the low frequency mode in liquid CS₂ is mainly originated in the molecular libration. It is also reported in time resolved impulsive stimulated scattering measurements that the librational motion of CS₂ molecule become prominent at high pressures.¹⁴ In the Raman result the width of vibrational density of states calculated from the Raman spectrum increases with pressure, while its peak frequency approaches to the libration frequency of the crystal. This behavior is understandable because the structure of liquid CS₂ at high pressure maintains its hard core liquidlike properties as shown above. The direction of this change is essentially different from crystallization and does not decrease the inhomogeneity significantly. Therefore the increase of the vibrational frequency with pressure should be explained as the hardening of the inter-molecular potential caused by the decrease of molecular separation, not as the molecular alignment directed toward crystal structure.

VI. CONCLUSIONS

We performed x-ray diffraction measurements on liquid carbon disulfide up to the pressure just below the freezing point and obtained the following conclusions. First, the changes in local configuration in liquid structure occurs below 0.3 GPa and then the structure changes rather similarly up to the freezing pressure. Second, the obtained structure function is basically explained as a simple liquid with Lennard-Jones type interaction at all pressures as justified by the coincidence with the MD simulation results. Third, the liquid structure has crystallike local structure but it approaches to monoatomic hard core liquid as the intermolecular sulfur-sulfur distance approaches to the intramolecular sulfur-sulfur distance. This trend explains why the width of the vibrational density of states increases with pressure.

- ¹N. C. Baenziger and W. L. Duax, *J. Chem. Phys.* **48**, 2974 (1968).
- ²C. E. Weir, G. J. Piermarini, and S. Block, *J. Chem. Phys.* **50**, 2089 (1969).
- ³Y. Fujita and S. Ikawa, *J. Chem. Phys.* **103**, 9580 (1995).
- ⁴Y. Fujita and S. Ikawa, *J. Chem. Phys.* **103**, 3907 (1995).
- ⁵Y. N. F. Yuan, R. A. Eaton, and A. Anderson, *Chem. Phys. Lett.* **269**, 305 (1997).
- ⁶A. Ishizumi, S. Yamamoto, and J. Nakahara, *J. Lumin.* **94–95**, 687 (2001).
- ⁷J. Watanabe, Y. Watanabe, M. Tango, and S. Kinoshita, *J. Lumin.* **87–89**, 779 (2000).
- ⁸C. Kalpouzos, D. McMorrow, W. T. Lotshaw, and G. A. Kenney-Wallace, *Chem. Phys. Lett.* **150**, 138 (1988).
- ⁹I. A. Heisler, R. R. B. Correia, T. Backup, S. L. S. Cunha, and N. P. da Silveira, *J. Chem. Phys.* **123**, 54509 (2005).
- ¹⁰T. Steffen, N. A. C. M. Meinders, and K. Duppen, *J. Phys. Chem.* **102**, 4213 (1998).
- ¹¹B. I. Greene and R. C. Farrow, *Chem. Phys. Lett.* **98**, 273 (1983).
- ¹²S. Kinoshita, Y. Kai, Y. Watanabe, and J. Watanabe, *J. Lumin.* **87–89**, 706 (2000).
- ¹³C. J. Fecko, J. D. Eaves, and A. Tokmakoff, *J. Chem. Phys.* **117**, 1139 (2002).
- ¹⁴B. Kohler and K. A. Nelson, *J. Phys. Chem.* **96**, 6532 (1992).
- ¹⁵R. P. Gardner and S. H. Lee, *Adv. X-Ray Anal.* **41**, 941 (1999).
- ¹⁶W. Guo, S. H. Lee, and R. P. Gardner, *Nucl. Instrum. Methods Phys. Res. A* **531**, 520 (2004).
- ¹⁷K. Nishikawa and T. Iijima, *Bull. Chem. Soc. Jpn.* **57**, 1750 (1984).
- ¹⁸K. Tamura, M. Inui, and S. Hosokawa, *Rev. Sci. Instrum.* **70**, 144 (1999).
- ¹⁹K. Funakoshi, Ph.D. thesis, Tokyo Institute of Technology, 1997.
- ²⁰N. Norman, *Acta Crystallogr.* **10**, 370 (1957).
- ²¹J. Krogh-Moe, *Acta Crystallogr.* **9**, 951 (1956).
- ²²P. J. Brown, A. G. Fox, E. N. Maslen, A. O'Keefe, T. M. Sabine, and B. T. M. Willis, *International Tables for Crystallography C* (Kluwer Academic, Dordrecht, 1992), p. 475.
- ²³S. I. Sandler and A. H. Narten, *Mol. Phys.* **32**, 1543 (1976).
- ²⁴S. Ikawa and E. Whalley, *J. Chem. Phys.* **85**, 2538 (1986).
- ²⁵H. Shimizu, S. Sasaki, and T. Ishidate, *J. Chem. Phys.* **86**, 7189 (1987).
- ²⁶W. Bridgman, *Proc. Am. Acad. Arts Sci.* **74**, 399 (1942).
- ²⁷H. J. C. Berendsen, D. van der Spoel, and R. van Drunen, *Comput. Phys. Commun.* **91**, 43 (1995).
- ²⁸E. Lindahl, B. Hess, and D. van der Spoel, *J. Mol. Model.* **7**, 306 (2001).
- ²⁹S. B. Zhu, J. Lee, and G. W. Robinson, *Mol. Phys.* **65**, 65 (1988).
- ³⁰T. Iijima and K. Nishikawa, *J. Mol. Struct.* **352/353**, 213 (1995).
- ³¹M. M. Thiéry and C. Rérat, *J. Chem. Phys.* **122**, 44503 (2005).
- ³²Y. Akahama, Y. Minamoto, and H. Kawamura, *J. Phys.: Condens. Matter* **14**, 19457 (2002).
- ³³D. J. Tildesley and P. A. Madden, *Mol. Phys.* **42**, 1137 (1981).
- ³⁴D. Chandler, *Annu. Rev. Phys. Chem.* **29**, 441 (1978).